JACS
JOURNAL OF THE AMERICAN CHEMICAL SOCIETY
pubs.acs.org/JACS
Communication

Directing Molecular Weaving of Covalent Organic Frameworks and Their Dimensionality by Angular Control

Xing Han, S. Ephraim Neumann, Brent L. Nannenga, Kaiyu Wang, Kelvin Kam-Yun Li, Saber Mirzaei, Xuan Yao, Chenhui Zhu, Mei-Yan Gao, Yue-Biao Zhang, Yong Cui, and Omar M. Yaghi*

Cite This: J. Am. Chem. Soc. 2023, 145, 22885−22889
Read Online

ABSTRACT: Although reticular chemistry has commonly utilized mutually embracing tetrahedral metal complexes as crossing points to generate three-dimensional molecularly woven structures, weaving in two dimensions remains largely unexplored. We report a new strategy to access 2D woven COFs by controlling the angle of the usually linear linker, resulting in the successful synthesis of a 2D woven pattern based on chain-link fence. The synthesis was accomplished by linking aldehyde-functionalized copper(I) bisphenanthroline complexes with bent 4,4′-oxydianiline building units. This results in the formation of a crystalline solid, termed COF-523-Cu, whose structure was characterized by spectroscopic techniques and electron and X-ray diffraction techniques to reveal a molecularly woven, twofold-interpenetrated chain-link fence. The present work significantly advances the concept of molecular weaving and its practice in the design of complex chemical structures.

Molecular weaving in two dimensions (2D) poses a significant challenge because the crossing points used as a "code" for interlacing are tetrahedral.[1−6] 2D woven patterns have garnered significant scientific interest,[7−9] and we have previously addressed this issue by using metal−organic helicates to produce 2D weaving patterns in the form of chicken wires.[10] In this contribution, we show how control of the angle between such crossing points gives the molecular analog of a very common 2D weaving pattern in society, namely, the chain-link fence (Figures 1 and S6).[11,12]

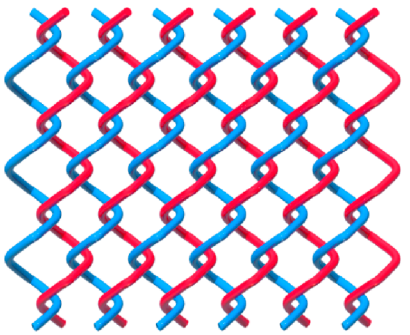

Figure 1. Mechanical entanglement in 2D woven COFs in the form commonly known as chain-link fence.

Our synthetic strategy is shown in Figure 2, in which an aldehyde-functionalized derivative of the complex salt bis[4,4′-(1,10-phenanthroline-2,9-diyl)bis([1,1′-biphenyl]-4-carbaldehyde)]copper(I) tetrafluoroborate, $Cu(PBC)_2BF_4$ is employed. The single-crystal structure of this complex reveals the position of the aldehyde groups to approximate a distorted tetrahedral geometry (Figure S1). The aldehyde functionalities of the distorted PBC ligand and the amino functionalities of 4,4′-oxydianiline (ODA) act as the points of extension for the formation of imine linkages. The 58.5° and 117.3° angles between the functional groups in PBC and ODA, respectively, complement each other to facilitate the generation four-membered helical PBC−ODA threads. The phenanthroline-based ligands are linked together by copper(I) ions in a mutually embracing manner. Each helical thread intertwines with two neighboring threads that are running parallel to each other to give an overall 2D molecular weaving framework (termed COF-523-Cu) resembling a chain-link fence.

The synthesis of COF-523-Cu $[Cu(PBC)_2(ODA)_2BF_4]_{imine}$ was carried out based on reversible imine bond formation. Equimolar amounts of $Cu(PBC)_2BF_4$ (25 mg, 0.02 mmol) and ODA (8.0 mg, 0.04 mmol) were reacted in a mixture of *n*-BuOH and chlorobenzene (1:1 v/v, 1 mL) in the presence of aqueous acetic acid (6 mol/L, 0.1 mL). The reaction mixture was sealed in a Pyrex tube and heated to 140 °C for a duration of 7 days. Upon completion, the precipitate was collected by centrifugation, and unreacted starting materials were removed by solvent extraction with anhydrous THF. The solvent was removed under dynamic vacuum at 120 °C for 12 h, producing 26 mg [82% yield based on $Cu(PBC)_2(BF_4)$] of COF-523-Cu as a dark-brown crystalline solid, which exhibited insolubility in typical polar and nonpolar organic solvents.

Fourier transform infrared spectroscopy (FTIR) and solid-state NMR spectroscopy studies were performed on COF-523-Cu to confirm the formation of imine linkages. The FTIR spectrum of COF-523-Cu showed a signal at 1621 cm^{-1}, which

Received: September 5, 2023
Published: October 16, 2023

https://doi.org/10.1021/jacs.3c09691
J. Am. Chem. Soc. 2023, 145, 22885−22889

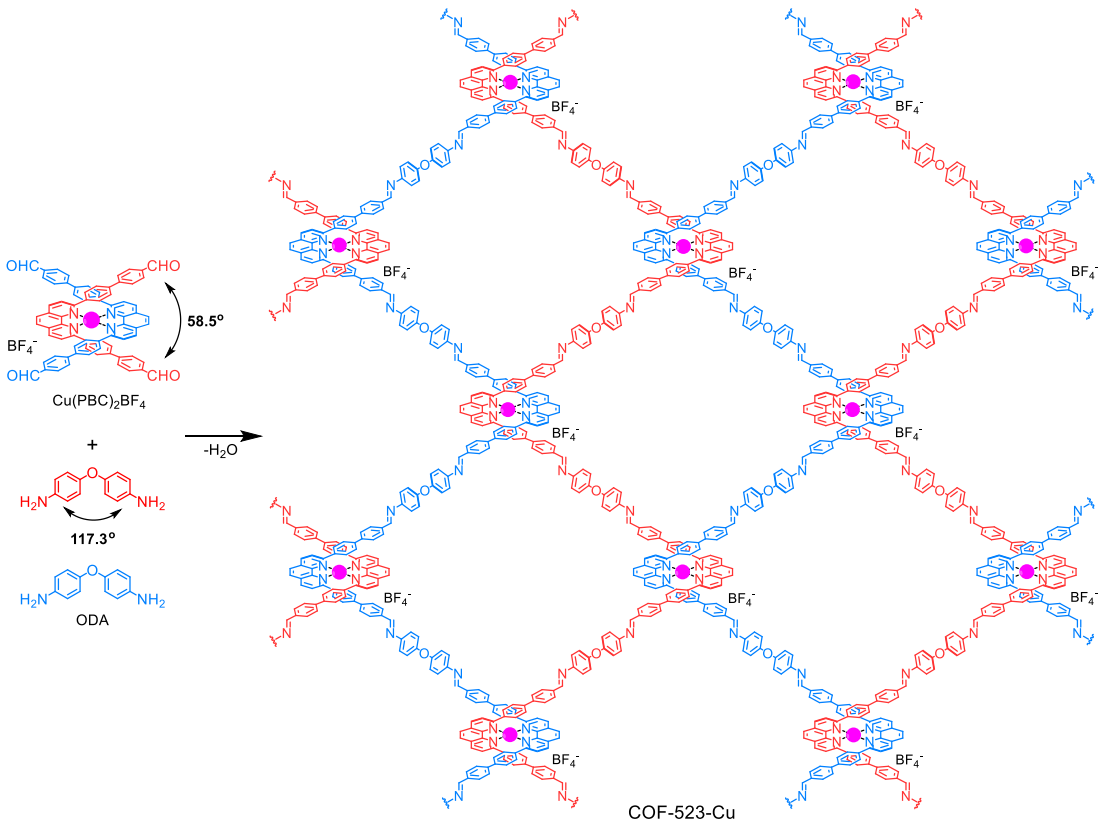

Figure 2. Synthetic strategy for constructing 2D woven COFs with bent linkers. $Cu(PBC)_2BF_4$ reacts with ODA to form COF-523-Cu. The interlacing threads are colored red and blue for clarity, and the copper crossing points are colored pink.

is characteristic of the C═N stretching modes for imine bonds (Figure S2). To better distinguish between the C═N double bonds of the phenanthroline units and the generated imine linkages in FT-IR and solid-state ^{13}C cross-polarization magic-angle spinning (CPMAS) NMR studies, a ^{13}C-labeled version of COF-523-Cu was synthesized by specifically labeling the imine position. A comparison between IR spectra of labeled and unlabeled samples (Figure S3) was based on treating the vibration normal modes as diatomic harmonic oscillators. The observed data aligned closely with the anticipated values derived from the assumption. Specifically, the $^{13}C{=}^{14}N$ stretch in the ^{13}C-labeled COF was detected at 1599 cm^{-1}, in contrast to the 1620 cm^{-1} absorption observed for the unlabeled variant. Similarly, the $^{12}C{=}^{16}O$ stretch present in the unlabeled $Cu(PBC)_2(BF_4)$ that appeared at 1690 cm^{-1} shifted to 1658 cm^{-1}. Further support for the presence of the imine linkage was obtained by solid-state ^{13}C CPMAS NMR analysis of labeled and unlabeled COF-523-Cu samples and a comparison to labeled $Cu(PBC)_2(BF_4)$ (Figure S4). In the unlabeled COF-523-Cu, definitively assigning the C═N carbon peaks was challenging due to the overlapping signals from the aromatic C═N bonds within the phenanthroline unit. The peak of the labeled aldehyde in $Cu(PBC)_2(BF_4)$ starting material was observed at around 195 ppm. In the labeled COF-523-Cu, the chemical shift around 195 ppm was significantly diminished, and a new prominent peak emerged at 159 ppm, which is attributed to the newly formed C═N carbon atoms. Overall, these observations served as initial confirmation of having covalently linked, extended threads in COF-523-Cu. Its thermal stability was studied by thermogravimetric analysis (TGA) measured under a N_2 atmosphere, and the onset of the thermal decomposition was found to be at ~350 °C (Figure S5), which is in good agreement with previously reported imine COFs.[13−17]

Scanning electron microscopy (SEM) micrographs show a homogeneous morphology of platelike crystals for COF-523-Cu with dimensions of approximately 1 μm × 1 μm × 0.1 μm (Figure 3b). A structural model of COF-523-Cu was constructed in Materials Studio 8.0 in the orthorhombic space group *P*222, which was subsequently used to index reflections observed in the powder X-ray diffraction (PXRD) pattern. The unit-cell parameters were further optimized by Pawley refinement of the experimental PXRD pattern to be a = 25.97 Å, b = 43.81 Å, c = 13.01 Å, and V = 14758.7 $Å^3$ with very low discrepancy factors (R_p = 0.93%, R_{wp} = 2.73%; Figure 3a). The calculated PXRD pattern of the modeled structure was found to be in good agreement with the experimental pattern of the activated COF-523-Cu. According to the refined model, COF-523-Cu crystallizes in a chain-link fence pattern of covalently linked 1D helical threads with a pitch of 26.0 Å (Figures 4a and S7) to construct a 3D pore system with channels of 16.5 Å × 26.0 Å.

The individual strands are mechanically braided and held by Cu(I) ions at each crossing point, thus forming a **wvx** net with 26.0 Å × 51.9 Å meshes along the crystallographic *c* axis. These 2D frameworks form a twofold-interpenetrating structure along the *a* direction and leave enough space for the BF_4^- counterion in the tunnels formed by the staggered stacking (AB stacking) of the layers along the *b* axis (Figures 4b and S7). In addition to the chain-link fence structure observed in COF-523-Cu, featuring a **wvx** net, other nets such as **wvy** and a three-dimensional structure with a fourfold **dia** topology can also be

https://doi.org/10.1021/jacs.3c09691
J. Am. Chem. Soc. 2023, 145, 22885−22889

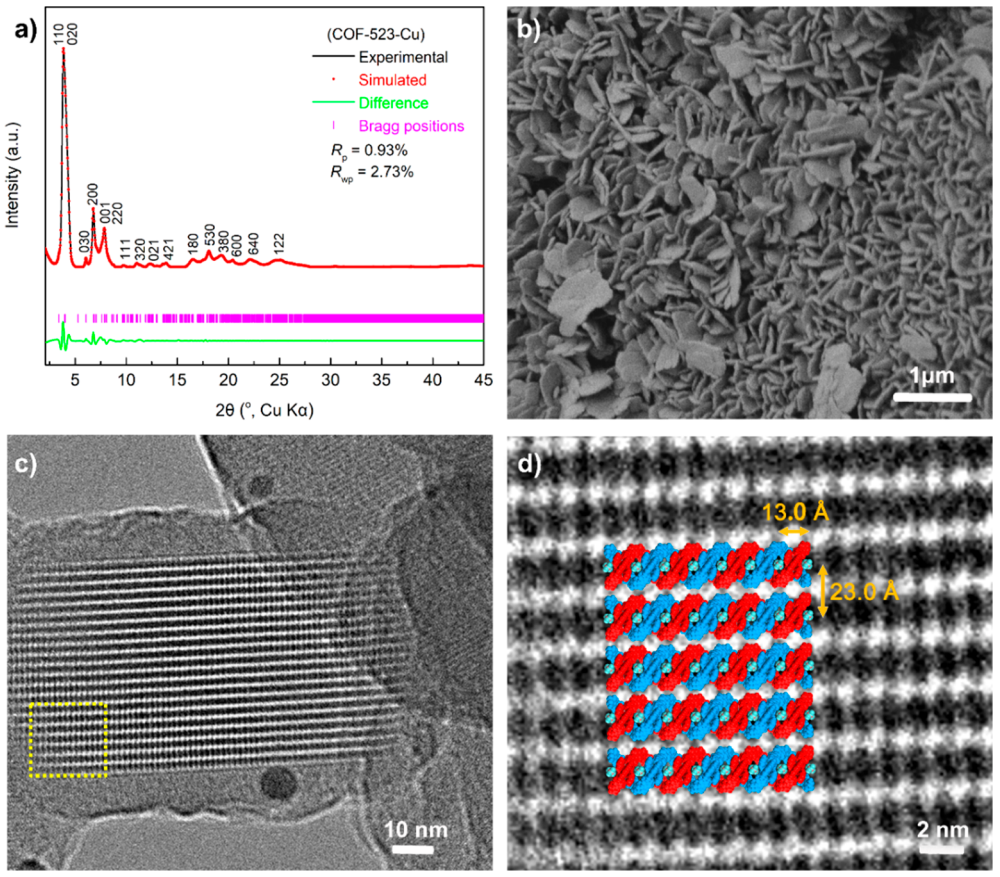

Figure 3. Structural characterization of COF-523-Cu. (a) Indexed PXRD pattern of the activated COF-523-Cu samples (black) and Pawley refinement (red) of the unit cell from the modeled structures. (b) SEM image of COF-523-Cu presenting platelike crystals. (c) High-resolution TEM image of COF-523-Cu taken along the [100] direction. (d) Magnified view of the highlighted area of (c) overlaid with a structure model showing good agreement along [100].

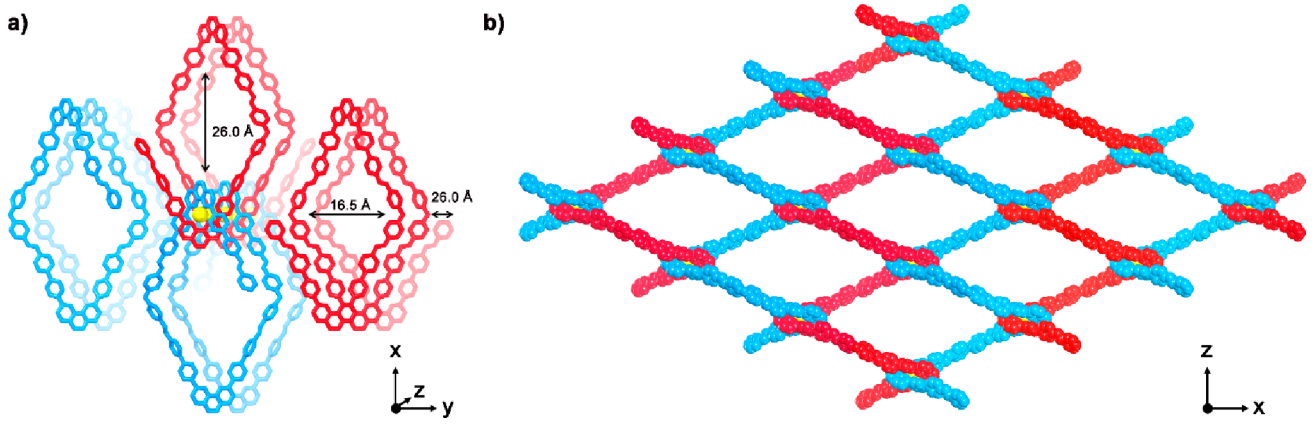

Figure 4. Crystal structure of COF-523-Cu. (a) The woven structure of COF-523-Cu consists of 1D helices with a pitch of 26.0 Å. The red and blue helices are identical and propagate with copper(I) ions at the crossing points. (b) COF-523-Cu formed by the weaving of adjacent parallel helical threads (blue and red) have a twofold-interpenetrating (not shown) 2D structure along the *b* direction. All hydrogen atoms and BF_4^- ions have been omitted for clarity. Copper atoms are shown in yellow.

plausible products.[18] Nevertheless, the simulated PXRD patterns for these structures are inconsistent with the experimental PXRD patterns obtained for COF-523-Cu (Figures S8 and S9). Following ultrasonication of the sample in ethanol, individual COF crystals were distributed on a copper sample grid for transmission electron microscopy (TEM) studies, which were conducted to procure additional insights into the crystal structure of COF-523-Cu (Figure 3c). Indeed, the overlay of the structural model with the experimentally obtained high-resolution TEM (HRTEM) images along [100] showed good agreement with the striped pattern of the lattice fringes observed in the HRTEM image. These fringes correspond to the (001) and (020) lattice planes, which are separated by 13.0 and 23.0 Å, respectively (Figure 3d). While COF-523-Cu consists entirely of homochiral helices within a single crystal domain, the presence of mixed

https://doi.org/10.1021/jacs.3c09691
J. Am. Chem. Soc. 2023, 145, 22885−22889

enantiomeric isomers results in an overall racemic woven structure. Both COF-523-Cu and COF-523 showed low N_2 uptake, and their BET surface areas are roughly estimated as 32 and 68 $m^2\ g^{-1}$, respectively (Figure S15). To test whether the pore space of the woven COF-523-Cu is guest-accessible, the structure was examined by tetrahydrofuran (THF) vapor adsorption at 283 K. COF-523-Cu exhibited an uptake of 59.6 $cm^3\ g^{-1}$ at P/P_0 = 0.90 (Figure S16). The hysteresis of the desorption is attributed to the solvated BF_4^- anions in the pores.[2]

Upon heating of the COF in a concentrated KCN solution of *n*-butanol/water (3:1), metal-free structures were obtained. The removal of 95−97% of the Cu(I) ions was confirmed using inductively coupled plasma atomic emission spectroscopy (ICP-AES). The dark-brown color of COF-523-Cu changed to pale yellow for the demetalated form, COF-523, as the demetalation proceeded (Figure S11). The crystallinity of COF-523 decreased drastically compared to the original COF-523-Cu, indicating spatial rearrangement of the structure and subsequent loss of long-range periodicity (Figure S12). As anticipated, the threads in COF-523 have significant freedom to shift either within or between layers without necessitating the breaking or bending of chemical bonds. In contrast to the reported 3D woven COFs, COF-523 does not regain crystallinity after reintroduction of Cu(I) ions (Figure S12). Nonetheless, the integrity of the overall structure is retained because of the constraints imposed by the mechanical weaving of the constituents: SEM images show similar morphologies before and after demetalation (Figure S14). Furthermore, the imine FTIR stretching vibration was retained at 1620 cm^{-1}, while the B−F stretching vibration at 1056 cm^{-1} disappeared (Figure S13). The removal of anions from the pores in the demetalated COF leads to an expected increase in THF uptake (Figure S16).

■ ASSOCIATED CONTENT

Supporting Information

The Supporting Information is available free of charge at https://pubs.acs.org/doi/10.1021/jacs.3c09691.

Detailed experimental section and characterization, including XRD, FTIR, solid-state NMR, and TGA (PDF)

Accession Codes

CCDC 2286467 ($Cu(PBC)_2BF_4$) and 2291988 (COF-523-Cu) contain the supplementary crystallographic data for this paper. These data can be obtained free of charge via www.ccdc.cam.ac.uk/data_request/cif, or by emailing data_request@ccdc.cam.ac.uk, or by contacting The Cambridge Crystallographic Data Centre, 12 Union Road, Cambridge CB2 1EZ, U.K.; fax: +44 1223 336033.

■ AUTHOR INFORMATION

Corresponding Author

Omar M. Yaghi − *Department of Chemistry and Kavli Energy Nanoscience Institute, University of California, Berkeley, California 94720, United States; Bakar Institute of Digital Materials for the Planet, College of Computing, Data Science, and Society, University of California, Berkeley, California 94720, United States; KACST−UC Berkeley Center of Excellence for Nanomaterials for Clean Energy Applications, King Abdulaziz City for Science and Technology, Riyadh 11442, Saudi Arabia;* orcid.org/0000-0002-5611-3325; Email: yaghi@berkeley.edu

Authors

Xing Han − *Department of Chemistry and Kavli Energy Nanoscience Institute, University of California, Berkeley, California 94720, United States; Bakar Institute of Digital Materials for the Planet, College of Computing, Data Science, and Society, University of California, Berkeley, California 94720, United States;* orcid.org/0000-0002-7921-8197

S. Ephraim Neumann − *Department of Chemistry and Kavli Energy Nanoscience Institute, University of California, Berkeley, California 94720, United States; Bakar Institute of Digital Materials for the Planet, College of Computing, Data Science, and Society, University of California, Berkeley, California 94720, United States;* orcid.org/0000-0002-8515-9621

Brent L. Nannenga − *Chemical Engineering, School for Engineering of Matter, Transport and Energy, Arizona State University, Tempe, Arizona 85287, United States; Center for Applied Structural Discovery, The Biodesign Institute, Arizona State University, Tempe, Arizona 85287, United States;* orcid.org/0000-0001-6859-3429

Kaiyu Wang − *Department of Chemistry and Kavli Energy Nanoscience Institute, University of California, Berkeley, California 94720, United States; Bakar Institute of Digital Materials for the Planet, College of Computing, Data Science, and Society, University of California, Berkeley, California 94720, United States*

Kelvin Kam-Yun Li − *Department of Chemistry and Kavli Energy Nanoscience Institute, University of California, Berkeley, California 94720, United States; Bakar Institute of Digital Materials for the Planet, College of Computing, Data Science, and Society, University of California, Berkeley, California 94720, United States*

Saber Mirzaei − *Department of Chemistry and Kavli Energy Nanoscience Institute, University of California, Berkeley, California 94720, United States; Bakar Institute of Digital Materials for the Planet, College of Computing, Data Science, and Society, University of California, Berkeley, California 94720, United States;* orcid.org/0000-0001-9651-9197

Xuan Yao − *Shanghai Key Laboratory of High-Resolution Electron Microscopy, School of Physical Science and Technology, ShanghaiTech University, Shanghai 201210, China*

Chenhui Zhu − *Advanced Light Source, Lawrence Berkeley National Laboratory, Berkeley, California 94720, United States*

Mei-Yan Gao − *Department of Chemistry and Kavli Energy Nanoscience Institute, University of California, Berkeley, California 94720, United States; Bakar Institute of Digital Materials for the Planet, College of Computing, Data Science, and Society, University of California, Berkeley, California 94720, United States;* orcid.org/0000-0001-6628-5190

Yue-Biao Zhang − *Shanghai Key Laboratory of High-Resolution Electron Microscopy, School of Physical Science and Technology, ShanghaiTech University, Shanghai 201210, China;* orcid.org/0000-0002-8270-1067

Yong Cui − *School of Chemistry and Chemical Engineering, Frontiers Science Center for Transformative Molecules and State Key Laboratory of Metal Matrix Composites, Shanghai Jiao Tong University, Shanghai 200240, China;* orcid.org/0000-0003-1977-0470

Complete contact information is available at: https://pubs.acs.org/10.1021/jacs.3c09691

Notes

The authors declare no competing financial interest.

■ ACKNOWLEDGMENTS

This research was supported by King Abdulaziz City for Science and Technology (KACST) as part of a joint KACST−UC Berkeley Center of Excellence for Nanomaterials for Clean Energy Applications and the Defense Advanced Research Projects Agency (DARPA) under Contract HR001-119-S-0048. The authors thank the University of California Berkeley Electron Microscope Laboratory for access and assistance in electron microscopy data collection. We thank Drs. Hasan Celik and Raynald Giovine and UC Berkeley's NMR facility in the College of Chemistry (CoC-NMR) for spectroscopic assistance. The instrument used in this work is supported by the National Science Foundation under Grant 2018784 and NIH S10OD024998. This research used resources of beamline 12.2.1 at the Advanced Light Source, which is a DOE Office of Science User Facility under Contract DE-AC02-4105CH11231. We acknowledge the use of the Titan Krios at the Erying Materials Center at Arizona State University and the funding of this instrument by NSF MRI 1531991. The authors thank Zichao Rong for helpful discussions.

■ REFERENCES

(1) Liu, Y.; Ma, Y.; Zhao, Y.; Sun, X.; Gándara, F.; Furukawa, H.; Liu, Z.; Zhu, H.; Zhu, C.; Suenaga, K.; Oleynikov, P.; Alshammari, A. S.; Zhang, X.; Terasaki, O.; Yaghi, O. M. Weaving of organic threads into a crystalline covalent organic framework. *Science* **2016**, *351* (6271), 365−369.

(2) Liu, Y.; Ma, Y.; Yang, J.; Diercks, C. S.; Tamura, N.; Jin, F.; Yaghi, O. M. Molecular Weaving of Covalent Organic Frameworks for Adaptive Guest Inclusion. *J. Am. Chem. Soc.* **2018**, *140* (47), 16015−16019.

(3) Liu, Y.; Diercks, C. S.; Ma, Y.; Lyu, H.; Zhu, C.; Alshmimri, S. A.; Alshihri, S.; Yaghi, O. M. 3D Covalent Organic Frameworks of Interlocking 1D Square Ribbons. *J. Am. Chem. Soc.* **2019**, *141* (1), 677−683.

(4) Zhao, Y.; Guo, L.; Gándara, F.; Ma, Y.; Liu, Z.; Zhu, C.; Lyu, H.; Trickett, C. A.; Kapustin, E. A.; Terasaki, O.; Yaghi, O. M. A Synthetic Route for Crystals of Woven Structures, Uniform Nanocrystals, and Thin Films of Imine Covalent Organic Frameworks. *J. Am. Chem. Soc.* **2017**, *139* (37), 13166−13172.

(5) Ma, T.; Zhou, Y.; Diercks, C. S.; Kwon, J.; Gándara, F.; Lyu, H.; Hanikel, N.; Pena-Sánchez, P.; Liu, Y.; Diercks, N. J.; et al. Catenated covalent organic frameworks constructed from polyhedra. *Nat. Synth.* **2023**, *2* (3), 286−295.

(6) Xu, H.-S.; Luo, Y.; Li, X.; See, P. Z.; Chen, Z.; Ma, T.; Liang, L.; Leng, K.; Abdelwahab, I.; Wang, L.; Li, R.; Shi, X.; Zhou, Y.; Lu, X. F.; Zhao, X.; Liu, C.; Sun, J.; Loh, K. P. Single crystal of a one-dimensional metallo-covalent organic framework. *Nat. Commun.* **2020**, *11* (1), 1434.

(7) Lewandowska, U.; Zajaczkowski, W.; Corra, S.; Tanabe, J.; Borrmann, R.; Benetti, E. M.; Stappert, S.; Watanabe, K.; Ochs, N. A. K.; Schaeublin, R.; Li, C.; Yashima, E.; Pisula, W.; Müllen, K.; Wennemers, H. A triaxial supramolecular weave. *Nat. Chem.* **2017**, *9* (11), 1068−1072.

(8) August, D. P.; Dryfe, R. A. W.; Haigh, S. J.; Kent, P. R. C.; Leigh, D. A.; Lemonnier, J.-F.; Li, Z.; Muryn, C. A.; Palmer, L. I.; Song, Y.; Whitehead, G. F. S.; Young, R. J. Self-assembly of a layered two-dimensional molecularly woven fabric. *Nature* **2020**, *588* (7838), 429−435.

(9) Wang, Z.; Błaszczyk, A.; Fuhr, O.; Heissler, S.; Wöll, C.; Mayor, M. Molecular weaving via surface-templated epitaxy of crystalline coordination networks. *Nat. Commun.* **2017**, *8* (1), 14442.

(10) Han, X.; Ma, T.; Nannenga, B. L.; Yao, X.; Neumann, S. E.; Kumar, P.; Kwon, J.; Rong, Z.; Wang, K.; Zhang, Y.; et al. Molecular weaving of chicken-wire covalent organic frameworks. *Chem* **2023**, *9* (9), 2509−2517.

(11) Nguyen, H. L.; Gropp, C.; Ma, Y.; Zhu, C.; Yaghi, O. M. 3D Covalent Organic Frameworks Selectively Crystallized through Conformational Design. *J. Am. Chem. Soc.* **2020**, *142* (48), 20335−20339.

(12) Gui, B.; Xin, J.; Cheng, Y.; Zhang, Y.; Lin, G.; Chen, P.; Ma, J.-X.; Zhou, X.; Sun, J.; Wang, C. Crystallization of Dimensional Isomers in Covalent Organic Frameworks. *J. Am. Chem. Soc.* **2023**, *145* (20), 11276−11281.

(13) Wang, Y.; Liu, Y.; Li, H.; Guan, X.; Xue, M.; Yan, Y.; Valtchev, V.; Qiu, S.; Fang, Q. Three-Dimensional Mesoporous Covalent Organic Frameworks through Steric Hindrance Engineering. *J. Am. Chem. Soc.* **2020**, *142* (8), 3736−3741.

(14) Zhai, L.; Cui, S.; Tong, B.; Chen, W.; Wu, Z.; Soutis, C.; Jiang, D.; Zhu, G.; Mi, L. Bromine-Functionalized Covalent Organic Frameworks for Efficient Triboelectric Nanogenerator. *Chem. - Eur. J.* **2020**, *26* (26), 5784−5788.

(15) Halder, A.; Ghosh, M.; Khayum M, A.; Bera, S.; Addicoat, M.; Sasmal, H. S.; Karak, S.; Kurungot, S.; Banerjee, R. Interlayer Hydrogen-Bonded Covalent Organic Frameworks as High-Performance Supercapacitors. *J. Am. Chem. Soc.* **2018**, *140* (35), 10941−10945.

(16) Chandra, S.; Kandambeth, S.; Biswal, B. P.; Lukose, B.; Kunjir, S. M.; Chaudhary, M.; Babarao, R.; Heine, T.; Banerjee, R. Chemically Stable Multilayered Covalent Organic Nanosheets from Covalent Organic Frameworks via Mechanical Delamination. *J. Am. Chem. Soc.* **2013**, *135* (47), 17853−17861.

(17) Ascherl, L.; Sick, T.; Margraf, J. T.; Lapidus, S. H.; Calik, M.; Hettstedt, C.; Karaghiosoff, K.; Döblinger, M.; Clark, T.; Chapman, K. W.; Auras, F.; Bein, T. Molecular docking sites designed for the generation of highly crystalline covalent organic frameworks. *Nat. Chem.* **2016**, *8* (4), 310−316.

(18) O'Keeffe, M.; Peskov, M. A.; Ramsden, S. J.; Yaghi, O. M. The Reticular Chemistry Structure Resource (RCSR) Database of, and Symbols for, Crystal Nets. *Acc. Chem. Res.* **2008**, *41* (12), 1782−1789.